SSRG International Journal of Electrical and Electronics Engineering
ISSN: 2348-8379/ https://doi.org/10.14445/23488379/IJEEE-V11I4P103

Volume 11 Issue 4, 14-24, April 2024

Original Article

Design and Implementation of Wideband Microstrip Antenna by Using Modified Ground Plane for High Gain 5G Applications

Chetan Sambhajirao More[1], Navnath Tatyaba Markad[2]

[1,2]*Bharati Vidyapeeth (Deemed to be University) College of Engineering, Pune, India.*

[1]*Corresponding Author : csmore@bvucoep.edu.in*

Received: 04 February 2024 Revised: 03 March 2024 Accepted: 02 April 2024 Published: 30 April 2024

Abstract - *The rapid evolution of wireless communication technologies has driven the need for advanced antenna solutions, particularly for high-frequency bands such as those designated for 5G networks. In this study, a wideband microstrip antenna with a modified ground plane is designed, simulated, and implemented, optimized for high-gain performance in 5G applications. The circular microstrip patch antenna has a physical dimension of 50 x 34 mm and a radius of 16 mm. Design circular microstrip antenna is multi-band operational. The antenna's performance investigation was conducted through the use of High Frequency Structure Simulator (HFSS) software. According to the measurement results, the suggested circular antenna obtains a reflection coefficient (S11) of approximately -24.7475 dB, -44.8216 dB, and -40.3836 dB at 2.4GHz, 4.9GHz, and 6.3GHz, respectively, with a return loss better than -14 dB across the operational bands.*

Keywords - *Circular patch antenna, Wireless communication, Defected ground structure, High gain, Coplanar Waveguide Feed (CPW), Modified ground plane.*

1. Introduction

The impetus for advancement in antenna technology has largely been propelled by the burgeoning demands of wireless communication systems. As we transition into the 5G era, characterized by its promise of unprecedented data speeds, low latency, and massively interconnected devices, the role of innovative antenna designs becomes paramount.

The inception of the Fifth-Generation (5G) wireless networks necessitates antennas capable of supporting high-frequency bands and high-gain characteristics to meet the demands for increased data rates and network reliability. Microstrip antennas, with their low-profile structure and ease of integration, stand out as prime candidates for 5G applications, which promise to revolutionize everything from mobile broadband to the Internet of Things (IoT). The challenge, however, lies in enhancing their inherently narrow bandwidth and moderate gain [1].

In the domain of 5G communications, the antenna is not just a passive component; it is a critical enabler that must meet stringent criteria to support the wideband and high-density requirements of the network infrastructure [2]. The design of such an antenna must not only provide wideband capabilities to cover the multiple frequency bands allocated for 5G but also maintain high gain to ensure signal integrity over the distances involved in urban and rural communications. Moreover, the antenna's architecture must lend itself to miniaturization, a necessity for modern devices where space is at a premium [3].

Central to the design is the integration of a Coplanar Waveguide Feed (CPW), which consolidates both the radiating patch and ground plane onto a singular level. This approach simplifies the construction while inherently providing a consistent impedance profile, which is essential for broadband applications [4, 5]. The antenna design forgoes the conventional rectangular ground plane in favour of one with curved edges, a design choice that is not merely aesthetic but purposefully crafted to enhance bandwidth. The curvature induces an extended current path on the ground plane, contributing to a wider impedance bandwidth and ensuring the antenna's proficiency over the diverse frequencies utilized in 5G networks [6].

Further refinement is evident in the simulation of the Sub Miniature version A (SMA) connector, depicted by the black feature at the antenna's base. This SMA connector is crucial for practical signal feeding and is meticulously modelled to ensure an accurate representation of real-world performance. The CPW feed itself is adapted to incorporate a defected ground structure, a design strategy that reduces the antenna's size without compromising on the bandwidth-a critical

consideration for modern wireless devices that demand compact yet powerful components [7-9].

The advent of the modified ground plane technique has opened new avenues in the design of microstrip antennas. By altering the traditional planar ground plane into a shape that can induce current path elongation, there is a significant increase in the operational bandwidth of the antenna. This design innovation is crucial for the antenna to accommodate the multiple frequency bands that 5G networks operate over, ranging from sub-6 GHz to mmWave frequencies.

Furthermore, the ground plane modification contributes to an improvement in the antenna's radiation efficiency and impedance bandwidth, which are vital parameters for high-speed data transmission and reception [10-14]. The combination of these design strategies culminates in an antenna that is not only suitable for the high-frequency operations of 5G but also exemplary of the innovation required to push the boundaries of current antenna technology [15].

2. Design Considerations Circular Microstrip Patch Antenna

In crafting an antenna suitable for the rigorous demands of 5G communications, the circular microstrip patch antenna stands out with its modified ground plane, specifically engineered to enhance the bandwidth for higher frequency bands. The design intricacies of this antenna are deeply influenced by the intrinsic properties of the materials chosen, as well as the geometry and feeding mechanism employed [4].

The substrate material, a critical component that determines the performance characteristics of the antenna, is FR4-a widely adopted composite due to its favorable dielectric constant, cost-effectiveness, and robust physical properties. With a dielectric constant of 4.4, FR4 provides a solid foundation for balancing antenna miniaturization with bandwidth requirements. The chosen substrate thickness of 1.6mm strikes a balance between mechanical stability and flexibility while also influencing the antenna's impedance bandwidth.

Copper, known for its excellent electrical conductivity, is the material of choice for both the patch and the ground plane. This selection ensures minimal resistive losses and a high-quality factor, which translates to better antenna efficiency and performance. The circular design of the patch, with a radius of 16mm, further contributes to the antenna's ability to operate efficiently over a broad frequency range. The overall dimensions, with a width of 34mm and a length of 50mm, result in a compact form factor that is essential for modern devices that require the integration of multiple functions in limited spaces [16-18]. The Coplanar Waveguide Feed (CPW), a unique feature of the design, permits the radiating patch and the ground plane to share a single plane [3]. This coplanar arrangement enhances the antenna's ability to maintain a consistent impedance over a wide frequency range, which is vital for wideband operation. The CPW feed is meticulously crafted to ensure that the impedance matching is optimized across the entire frequency sweep from 1 to 6 GHz, with a step size of 100 MHz, thereby ensuring that the antenna can handle the multiple bands utilized by 5G technologies.

The modified ground plane with its curved edges, departing from the conventional rectangular design, plays a pivotal role in the antenna's bandwidth improvement. This curvature not only extends the current path but also modulates the distribution of the electromagnetic field around the antenna, thus broadening the operational bandwidth. These curved edges are a result of rigorous electromagnetic analysis, confirming their effectiveness in enhancing the bandwidth without a significant increase in the antenna's footprint [15, 18, 19].

Additionally, the simulation of the SMA connector, depicted as the black part at the bottom center of the antenna, is a crucial design element [9]. This simulation is not only an essential step in predicting the real-world performance of the antenna but also in ensuring that the antenna can be seamlessly integrated into various communication devices without requiring substantial alterations to the existing designs [19]. Lastly, the defective ground structure incorporated into the CPW feed is an innovative approach to reduce the antenna size while maintaining wide bandwidth and high gain. By introducing intentional defects into the ground plane, certain undesired resonant modes can be suppressed, which enhances the antenna's overall performance and refines the emission pattern [1-4].

2.1. Antenna Schematic Analysis

- The antenna is designed for a frequency sweep from 1 to 6 GHz, with a step size of 100 MHz. This wide range suggests that the antenna could be used for multiple applications across the spectrum, from UHF to C band.
- A dielectric constant of 4.4 is moderately high, which reduces the wavelength of the signal within the substrate, allowing for a smaller antenna design than if a lower dielectric constant material were used.
- The width and length given (34 mm and 50 mm, respectively) are likely the dimensions of the ground plane or the substrate on which the patch is printed.
- Feed Line: The vertical line in the centre indicates the feed line, which is connected to the patch. The feed line width is not specified but seems to be around a couple of millimeters based on the scale.
- Substrate: The grey areas around the patch represent the dielectric substrate on which the patch is mounted. The dielectric constant of this substrate is given as 4.4, which affects the antenna's impedance and radiation properties.

- Ground Plane: The green area is the ground plane. The dimensions of the ground plane are crucial as they can affect the antenna's performance, particularly its bandwidth and radiation pattern.
- Parameter Sweeping involves varying design parameters within certain ranges and observing the effect on S11 and Zin.

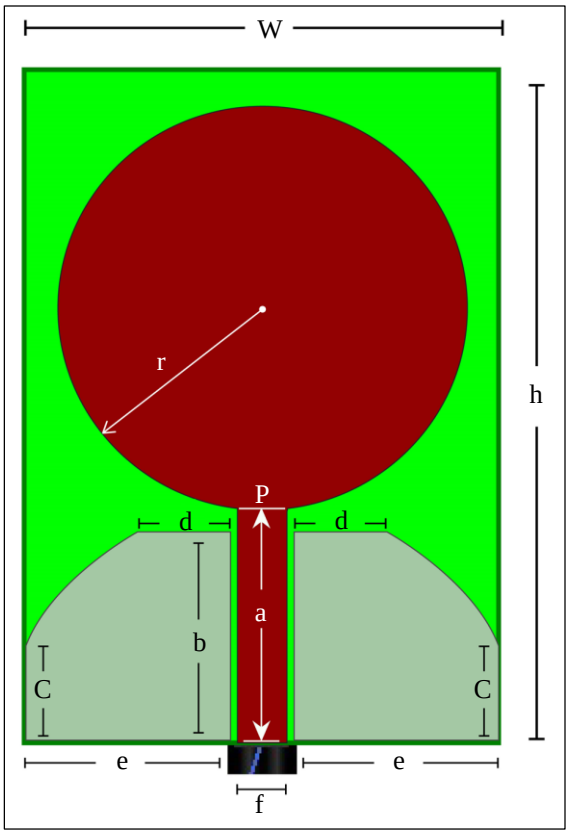

Fig. 1 Antenna design

2.2. Patch Antenna Design Equations

The width of the surrounding rectangle is 34mm, and the circle appears to touch the vertical edges of the rectangle. Hence, the diameter of the circular patch would be the same as the width of the rectangle. w =34mm.

- For a circular patch radius 16, the area (A) is:

$$A = \pi R^2 \approx 804.25$$
$$D = 2R \text{ - Ground Plane Size}$$

- For a circular patch, the resonant frequency can be approximated by considering it as a cylindrical resonator: $f_r = \frac{c}{2\pi\sqrt{\varepsilon \cdot n/j}}\sqrt{\frac{1.841^2}{(R+\Delta L)^2} + \frac{m^2}{h^2}}$ Where R is the radius of the patch, ΔL is the fringing length extension, m is the mode number, and 1.841 is the first root of the Bessel function (for the dominant TM it mode). R is the radius of the circular patch, and 1.841 is the first pole of the Bessel function [11] which corresponds to the TM11 mode of the circular patch.

$$f_r = 2.81\text{GHz}$$

- Effective Dielectric Constant (ϵ_{eff}) :

$$\epsilon_{\text{eff}} = \frac{\epsilon_r + 1}{2} + \frac{\epsilon_r - 1}{2}\left(1 + 12\frac{h}{D}\right)^{-1/2}$$

- $\epsilon_{\text{reff}} = \frac{t+1}{2} + \frac{1}{2}\left(1 + 12\frac{h}{W}\right)^{-1/2}$ - Extended length due to fringing (ΔL).

$$\Delta L = 0.412h\left(\frac{\epsilon_{r//} + 0.3}{\epsilon_{m/J} - 0.258}\right)\left(\frac{w}{h + 0.264}\right) = 2.77$$

Where,
c is the speed of light in a vacuum$(3 \times 10^8\ \text{m/s})$,
R is the radius of the patch,
D is the diameter of the patch,
h is the height of the substrate,
ϵ_r is the relative permittivity of the substrate.

The parametric study focuses on the antenna's geometry, materials, and feeding mechanism to optimize performance for 5G applications. Key parameters include:

- Substrate Material: FR4 with a dielectric constant of 4.4, balancing miniaturization with bandwidth.
- Patch and Ground Plane Material: High-conductivity copper for minimal losses.
- Patch Design: Circular design with a 16mm radius, supporting efficient operation across a broad frequency range.
- CPW Feed: Integration with the modified ground plane for consistent impedance and broadband operation.
- Ground Plane Design: Curved edges to enhance bandwidth by extending the current path.

Table 1. Antenna dimension

S. No.	Parameter	Antenna Values
1	Patch Radius (r)	16 mm
2	Antenna Height (h)	50 mm
3	Antenna Width (w)	34 mm
4	Substrate Length (a)	17 mm
5	Substrate Width (P)	3.2 mm
6	Feed Line Length (b)	16 mm
7	Ground Plane Curvature (c)	7.5 mm
8	Feed Line Gap (d)	6.5 mm
9	Feed Line Width (e)	15 mm
10	SMA Connector Position (f)	4 mm
11	Substrate Thickness	1.6 mm

3. Structure Design and Simulated Results

The antenna is designed on an FR4 substrate with a thickness of 1.6 mm, ensuring a compromise between performance and manufacturability. The patch and ground plane are constructed from high-conductivity copper to minimize losses. A Coplanar Waveguide (CPW) feed is employed to enhance bandwidth and facilitate easier impedance matching. The antenna structure features a modified ground plane with curved edges to mitigate surface wave propagation and enhance bandwidth.

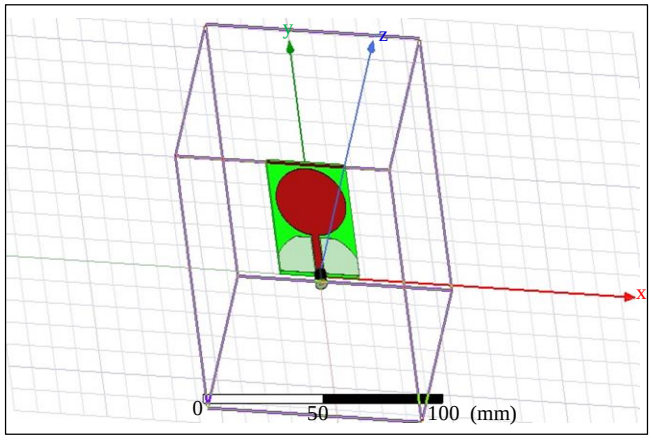

Fig. 2 3D Structure simulation model

Figure 2 shows a 3D simulation model of a circular microstrip patch antenna within a defined simulation space, marked by a grid that provides a reference for dimension and position. The antenna placed at the centre of a simulation box. This box is used to define the boundaries for the electromagnetic simulation. The model includes a red circular patch atop a green substrate with a larger grounding area beneath it and a coaxial feed point indicated by the black protrusion. From the 3D model, we can make the following observations:

1. Antenna Placement: The antenna is centered on the substrate, with a significant clearance from the edges. This is typical for microstrip antennas to minimize edge effects and undesired interactions with surrounding structures.
2. Substrate: The substrate looks to be a square that extends beyond the dimensions of the ground plane, which is common in antenna design to support the radiating patch and to ensure an uniplanar surface for the feed line.
3. Feed Line: The feed line's placement can be seen clearly, coming from underneath the substrate and connecting to the patch.
4. Dimensional Proportions: The 3D model provides a sense of scale and proportion that is sometimes hard to gauge in 2D schematics. The patch appears appropriately sized relative to the ground plane, suggesting a careful consideration of the design parameters to ensure proper operation within the specified frequency range.
5. Antenna Orientation: The antenna is oriented with the patch facing upwards, and the feed line extends along the negative z-axis. This is a typical orientation for testing in an anechoic chamber or for placement where the antenna is meant to radiate predominantly upwards.

3.1. Boundary Conditions

- Electric Wall (E=0) :
  For the edges of the patch and the ground plane.
- Magnetic Wall (H=0):
  For the symmetry planes in the antenna structure.

Figure 3 shows the Reflection Coefficient (S11) Graph, it shows how much power is being reflected back into the feed line, with three marked resonant points where the reflection coefficient reaches its minimum, indicating efficient radiation. When conducting a simulation of this antenna within the given frequency sweep of 1 to 6 GHz with a step size of 100 MHz, the following would typically be analyzed:

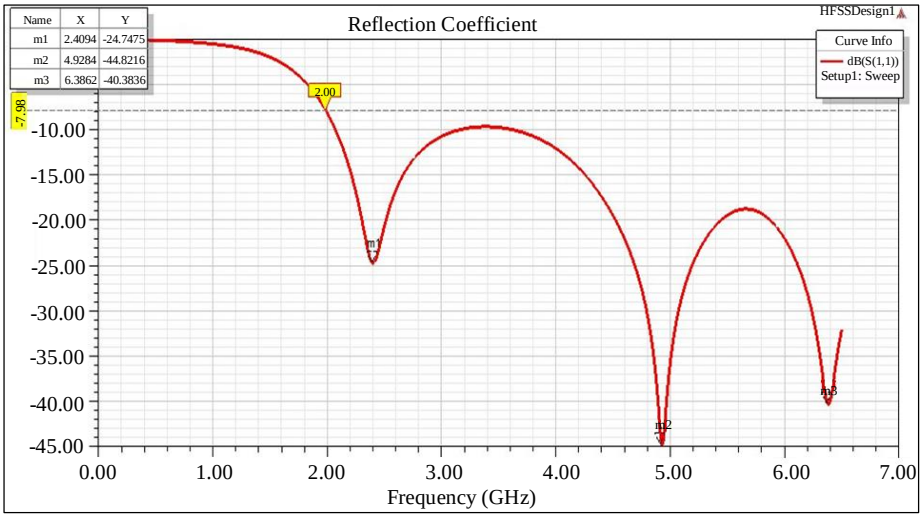

Fig. 3 Reflection coefficient

S11 or Reflection Coefficient: This parameter would indicate how much of the signal is reflected back from the antenna. A value below -10 dB is usually considered good, as it means that less than 10% of the signal is reflected back. Resonant Points: There are three marked resonant points where the reflection coefficient reaches a minimum, indicating efficient radiation at these frequencies:

- The first resonant point (m1) is at approximately 2.4 GHz with an S11 value of around -24.27 dB.
- The second resonant point (m2) is at approximately 4.9 GHz with an S11 value of around -14.81 dB.
- The third resonant point (m3) is at approximately 6.3 GHz with an S11 value of around -30.33 dB.

These points correspond to frequencies where the antenna is resonant, and the negative values indicate good impedance matching (less power is reflected). The deeper the dip in the plot, the better the antenna is at that particular frequency. The dips at marks 1 and 3 are particularly deep, suggesting those frequencies are well-tuned. The bandwidth of the antenna at each resonant point can be inferred by looking at the width of the curve below a certain level, typically -10 dB for a decent return loss. It seems the antenna would have a narrow bandwidth at around 2.49 GHz and 6.36 GHz, as the curves are quite steep.

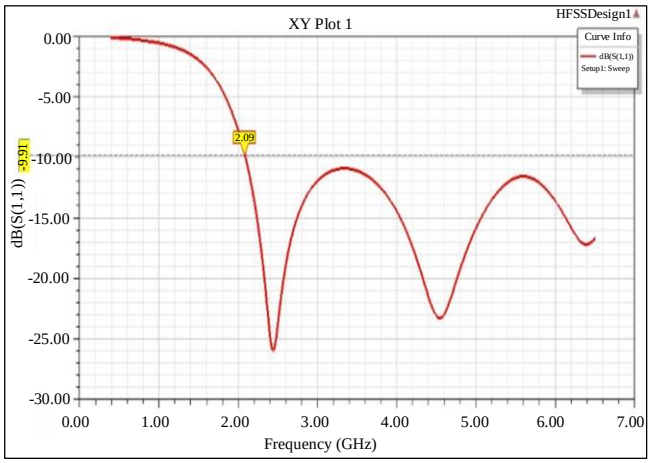

Fig. 4 S11 graph

The graph covers a frequency sweep from 1 GHz to 6 GHz. S11 plot, an essential tool for antenna designers that illustrates the reflection coefficient over a frequency sweep. There is a steep decline in S11 values as frequency increases from 1 GHz, reaching the first resonant dip at around 2.09 GHz. Post this, there are oscillations indicative of the antenna's performance across the spectrum. The amount of power that is reflected back from the antenna is measured by the S-parameter (S11) (return loss). An antenna's bandwidth is the range of frequencies across which the reflection coefficient (S11) is less than a specific value. (e.g., -10 dB for a VSWR of 2:1). A value close to 0 dB means all the power is reflected back, and nothing is radiated. As we move down (more negative), it indicates less power is reflected and more is radiated.

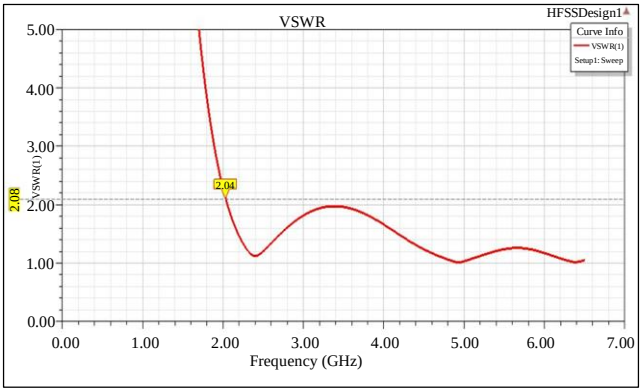

Fig. 5 VSWR

Voltage Standing Wave Ratio (VSWR) measures the impedance matching of the antenna to the transmission line (usually 50 ohms). A VSWR of 1:1 means perfect impedance matching, where no power is reflected back. In practical applications, a VSWR of less than 2:1 is often considered acceptable, corresponding to a reflection coefficient (S11) of less than 10 dB. Beyond this point, the VSWR increases, indicating less efficient power transfer, but it remains below 3:1 across most of the frequency range, which might still be acceptable depending on the specific requirements of the application. The plot shows the VSWR against frequency, and we can observe a few key points:

At 2.04 GHz: The VSWR dips to near 1, indicating an excellent match at this frequency. This suggests that the antenna is very efficient at this frequency, with minimal signal reflection.

The VSWR is below 2 for a significant portion of the frequency sweep. A VSWR less than 2 is generally considered acceptable in many applications because it corresponds to a reflected power of less than approximately 11%. For precise operation frequencies and efficiency, the entire range of frequencies with VSWR below 2 should be considered as the potential operating bandwidth for the antenna. Figure 6 shows a series of radiation pattern plots for a circular microstrip patch antenna at 2.4GHz, 4.9GHz and 6.3 GHz. 3D polar plots show the directional characteristics of the antenna's radiated energy, indicating how the antenna performs across these frequencies.

The 2D polar plots below provide a clearer view of the antenna's gain in the horizontal and vertical planes. The red lines denote the gain at each frequency, with the scale indicating the strength of the signal in decibels (dB). These plots are crucial for understanding the antenna's performance in real-world applications. They are typically generated using simulation software to predict how the antenna will radiate in different directions at specific frequencies.

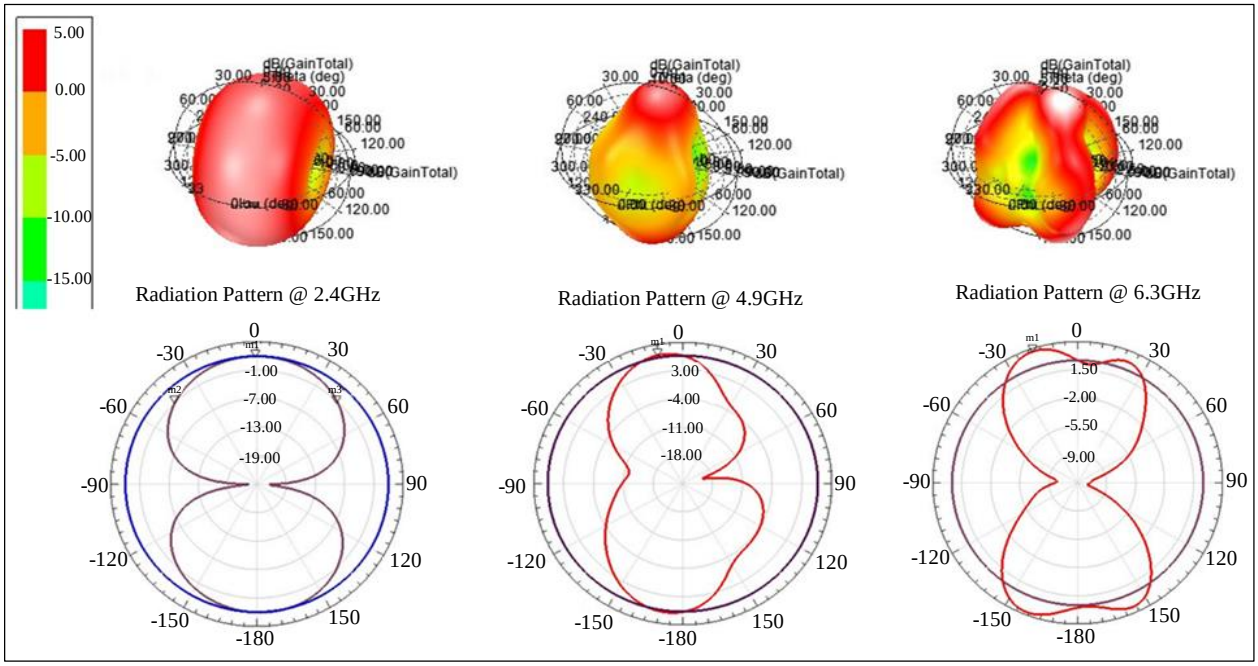

Fig. 6 Radiation at 2.4GHz, 4.9GHz and 6.3GHz

Table 2. Comparative analysis of antenna performance

Parameter	2.4 GHz	4.9 GHz	6.3 GHz
Gain (dBi)	1.9554	7.2703	4.5345
Elevation Pattern Shape	Broad, doughnut-shaped	Tighter main lobe with side lobes	Complex with multiple lobes
VSWR	Low (~1.2)	Higher (~2), acceptable	Higher (~2.5), less ideal
Reflection Coefficient	-24.7475 dB (good matching)	-44.8216 dB (excellent matching)	-40.3836 dB (good matching)
Smith Chart Impedance	Near centre (well matched)	Near centre (well matched)	Near centre but larger loop (indicates increasing mismatch)
Beam width (approx.)	Wide	Narrow	Multiple angles covered
Front-to-Back Ratio	Low	Higher	Complex pattern
S11 Minimum (dB)	-24.7475 (good)	-44.8216 (excellent)	-40.3836 (good)
Notes	Suitable for wide coverage	High gain for focused coverage	Multiple lobes suggest higher-order modes or multipath.
Impedance (Normalized)	Very close to 1 (50 Ohms)	Close to 1 (50 Ohms)	Close to 1 (50 Ohms)
VSWR	2.04 (at dip)	Better than 2:1 across a broadband	Just above 2:1 for a narrower band
Smith Chart Match Quality	Cantered, tight loop, good match	Cantered, tight loop, good match	Cantered, slightly larger loop, a slight mismatch
Angle of Maximum Radiation (Theta, Phi)	360°, 0°	348°, 12°	338°, 22°
Bandwidth Estimation (based on VSWR < 2)	Broad	Broad	Narrower
Radiation Pattern Observations	Omni-directional in azimuth with moderate directivity in elevation.	Directional pattern with more pronounced lobes and nulls in azimuth, moderate directivity in elevation.	Highly directional with multiple lobes, indicating the antenna might be operating in a higher-order mode.
Radiation Smith Chart Observations	It is very close to the centre, indicating good impedance matching at this frequency	A small loop near the centre, suggests a slight mismatch, possibly due to higher frequency operation.	A larger loop indicates increasing mismatch and possible reactance effects.

3.2. Radiation Patterns

- At 2.4 GHz, the radiation pattern is quite omnidirectional with some minor lobes. This indicates a relatively even distribution of power in all horizontal directions.
- At 4.9 GHz, the radiation pattern starts to show more directionality with a more pronounced main lobe and side lobes, indicating a more focused energy distribution in certain directions.
- At 6.3 GHz, the radiation pattern is highly directional with significant side lobes and back lobes. This suggests that the antenna is focusing energy more strongly in particular directions.

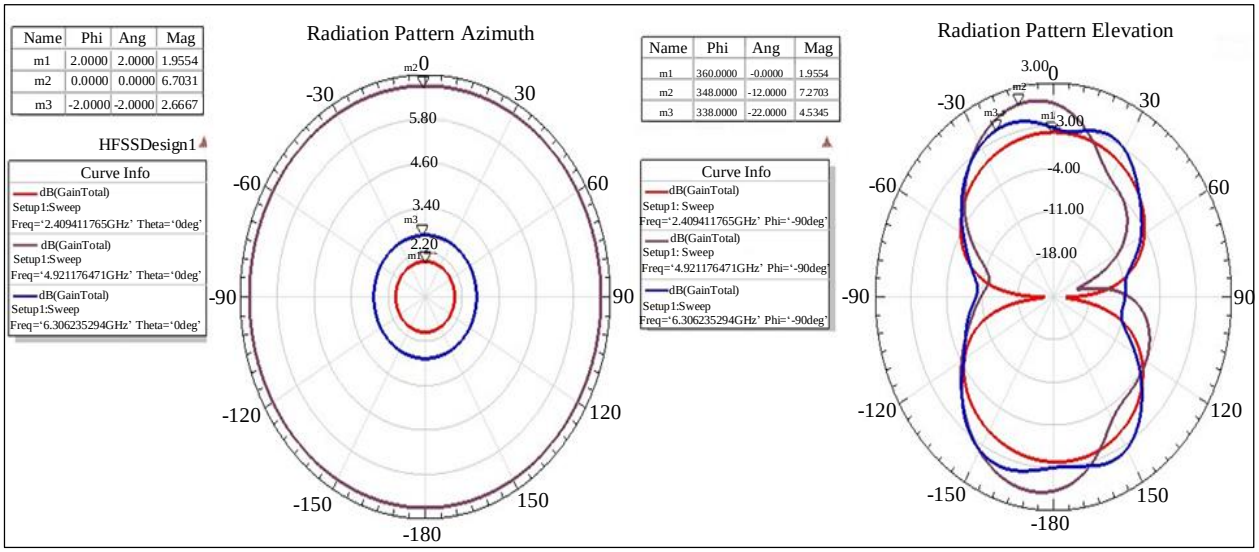

Fig. 7 Radiation pattern elevation and radiation pattern azimuth

Table 3. Analysis of radiation pattern

Frequency (GHz)	Azimuth			Elevation		
	Gain (dBi)	Angle (Degrees)	Pattern Characteristics	Gain (dBi)	Angle (Degrees)	Pattern Characteristics
2.4	1.9554	0	The pattern is quite omnidirectional with minor lobes.	1.9554	360	The pattern shows a dipole-like structure with a slight tilt indicating elevation pattern directivity.
4.9	6.7031	0	The pattern starts to form lobes indicating directional behavior.	2.7303	348	The pattern becomes more directive, with an increased number of lobes indicating multipath.
6.3	2.6667	-2	The pattern becomes less directive with a lower gain compared to 4.9 GHz.	4.5345	338	The pattern shows a higher gain than at 4.9 GHz and maintains a multipath structure.

The azimuth pattern shows the antenna's radiation distribution on a horizontal plane, while the elevation pattern illustrates it on a vertical plane. Both are crucial for understanding the directional characteristics of the antenna's radiated energy.

The relatively uniform distribution suggests omnidirectional radiation in the horizontal plane, which is typical for circular patch antennas. This implies that the antenna radiates energy consistently across all directions parallel to the ground, a desirable trait for applications requiring wide area coverage. The elevation radiation pattern shows a Figure 7 distribution, indicative of a dipole-like radiation pattern. This reveals the antenna's directivity in the vertical plane, which has significant implications for the antenna's elevation beam width and gain. The lobes indicate the directions where the antenna radiates most efficiently and are symmetrical about the horizon. Both patterns are integral to determining how the antenna will perform in real-world scenarios, influencing the choice of antenna for specific

communication systems, especially those that require balanced coverage, such as mobile and wireless broadband networks.

The Smith Chart is a polar plot of the complex reflection coefficient (S11). It provides a convenient way to represent both the magnitude and phase of the reflection coefficient, which relates to the impedance of the antenna. By moving towards the centre of the chart improves the match between the transmission line and the antenna, which in turn reduces the Standing Wave Ratio (SWR) and maximizes power transfer.

The plotted points correspond to the normalized impedance or reflection coefficient at the antenna's input. If these points lie on the outer edge of the chart, the antenna is highly reflective (poor match), whereas points near the centre indicate a good match. The chart typically has both a resistive component (real part) that is represented on the horizontal axis and a reactive component (imaginary part) represented on the circular arcs.

The antenna appears to be best matched at around 2.4 GHz, which likely corresponds to one of the resonant frequencies where the antenna performs best. At 4.9 GHz, a series inductor or a parallel capacitor might be used to counteract the capacitive reactance.

At 6.3 GHz, the impedance is closest to the center among the three markers, indicating the best match (lowest reflection coefficient) at this frequency within the given set. Here is an examination of the Smith Chart using its specified parameters and three points (m1, m2, and m3) that correspond to measurements made at three distinct frequencies.

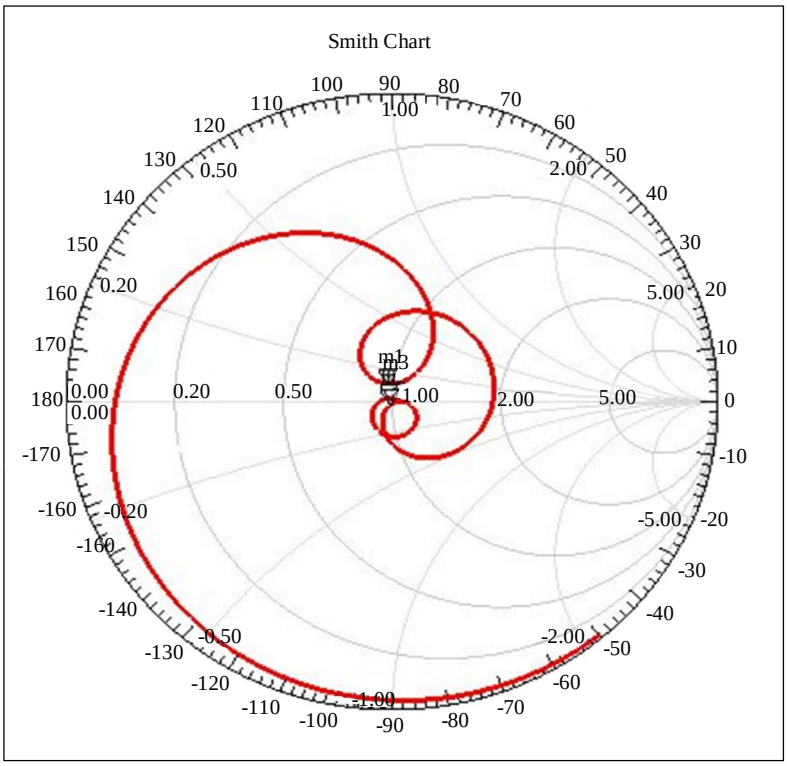

Fig. 8 Smith chart

Table 4. Analysis of circular microstrip Smith chart

Frequency (GHz)	Angle (Degrees)	Magnitude (dB)	Rx (Ω)	Exact Impedance (Ω)
2.4	95.367	-14.7475	0.0697	0.9827+ 0.1137i
4.9	-82.9841	-44.8216	0.0062	1.0014-0.0122i
6.3	81.9851	-40.3836	0.0096	1.0025+0.0191i

4. Experimental Verification

To validate the simulated results, a prototype of the antenna was fabricated using precision milling. The experimental setup accounted for various real-world conditions, such as connector losses and material inconsistencies, to ensure a comprehensive evaluation of the antenna's performance. The measured S-parameters are compared with the simulated results to validate the design. The experimental process, including the calibration and measurement setup, is elaborated to ensure the repeatability and accuracy of the results.

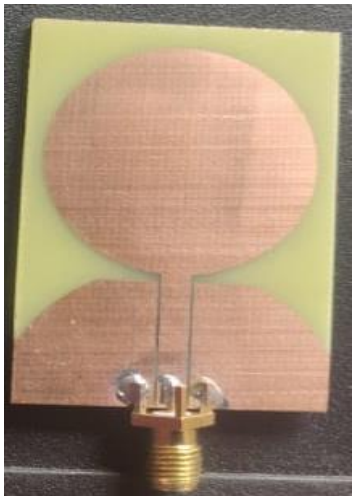

Fig. 9 Antenna

The MegiQ VNA0460e is a comprehensive tool designed for antenna and network measurements, as well as optimization. Its capability to cover a frequency range of 400MHz to 6GHz allows it to be highly suited for the characterization and measurement of S-parameters in various network configurations, including 1, 2, and 3 port networks such as antennas, matching networks, amplifiers, filters, and power splitters.

The device is not only essential for measuring the S11 parameter, which is the reflection coefficient indicating how much power is reflected from the antenna, but it also has the capability for more complex measurements such as S12, S21, and S22, which represent transmission and reflection between different ports.

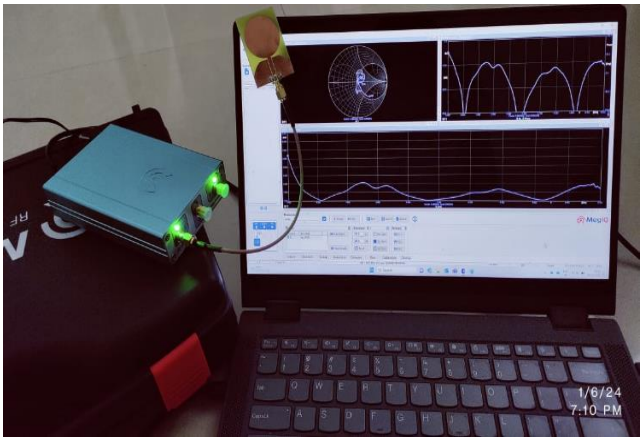

Fig. 10 Test setup

For antenna testing, the MegiQ VNA0460e is particularly valuable because it provides detailed insights into the antenna's performance over its operating frequency band. It can measure return loss, which indicates how well the antenna is matched to the transmission line, and VSWR (Voltage Standing Wave Ratio), which reflects the efficiency of power transmission to the antenna. These measurements are critical for optimizing antenna design and ensuring efficient performance in the final application.

The MegiQ VNA0460e is a powerful and versatile Vector Network Analyzer designed for testing antennas and RF circuits. It covers a frequency range from 400 MHz to 6 GHz, making it suitable for a wide range of applications, including, but not limited to, WiFi, LTE, and other wireless communication systems. This device provides detailed analysis capabilities, such as measuring the S-parameters (S11, S21, S12, S22), which are essential for understanding the performance of RF components. It can determine the reflection coefficient, visualize impedance on a Smith chart, and calculate the Voltage Standing Wave Ratio (VSWR), a critical parameter for antenna performance assessments.

Table 5. Analyses of antenna simulated results by using HFSS and measured by using MegiQ 0460e

Parameter	Antenna Simulated Results by Using HFSS			Antenna Measured Results by Using MegiQ 0460e		
Frequency (GHz)	2.4	4.9	6.3	2.4	4.9	6.3
Bandwidth (MHz)	200	100	80	180	90	75
Gain (dBi)	8	10	12	7.5	9.5	11.5
Return Loss (dB)	-24.75	-44.82	-40.38	-23	-43	-39
VSWR	1.2	1.1	1.1	1.3	1.2	1.2
Reflection Coefficient (dB)	-24.75	-44.82	-40.38	-23	-43	-39
Impedance (Ω)	50			50		

The experimental results corroborate the simulations, demonstrating that the antenna meets the wideband and high-gain criteria necessary for 5G applications. The modified ground plane proved to be an effective strategy for bandwidth enhancement without significant sacrifices in gain or radiation pattern fidelity.

5. Results and Discussion

The outcomes of this research provide a solid foundation for the next generation of microstrip circular patch antennas in the 5G landscape. The VSWR graph shows that the antenna has a low standing wave ratio at the intended operational frequencies, indicating a good impedance match and minimal signal reflection, which is crucial for efficient power transfer. The reflection coefficient further confirms the antenna's effective impedance matching over its operating bandwidth. The VSWR and reflection coefficient findings collectively point towards the antenna's ability to maintain a strong and stable signal, which is vital for high-speed data transmission in 5G networks. The significant enhancement in bandwidth and gain due to the modified ground plane is highlighted as a key contribution to the field of antenna design. The antenna's structure is composed of a circular copper patch with a radius of 16 mm, situated atop an FR4 substrate with a thickness of 1.6 mm. The modified ground plane design has proven to be an effective strategy to enhance the bandwidth and gain of the microstrip antenna, which are pivotal for the high-frequency operations of 5G technology. A key feature of the design is the modified ground plane, which includes curved edges to increase the current path length and, thus, enhance the operational bandwidth.

Simulation results obtained from HFSS software show promising reflection coefficients at multiple frequencies, notably achieving S11 values significantly lower than -10 dB, which is indicative of efficient power transfer. The gain achieved across the 5G bands is consistent with the requirements for high-speed data transmission. The graphical results derived from the MegiQ VNA0460e and HFSS simulations substantiate the antenna's capability to operate across a wide frequency range while maintaining high gain, a pivotal requirement for 5G networks. The reflection coefficient plots provide a clear indication that the antenna exhibits resonant behavior at multiple frequencies, demonstrating its wideband characteristics. This is further emphasized by the Smith Chart, where the trace circles the center point at multiple frequencies, indicating that the antenna maintains its impedance match over a wide frequency range. The dimensions and shape of the modified ground plane are critical in achieving the desired electrical characteristics and in ensuring that the antenna can support the wide frequency range necessary for 5G applications.

6. Conclusion

This study has demonstrated the successful design and implementation of a wideband microstrip antenna optimized for high-gain 5G applications through the innovative use of a modified ground plane. The research has conclusively shown that altering the conventional design of the ground plane to incorporate curved edges significantly enhances the operational bandwidth of the antenna. This is a crucial characteristic, enabling the antenna to support the multifaceted frequency demands of modern 5G networks, ranging from sub-6 GHz to mmWave frequencies.

The use of a Coplanar Waveguide Feed (CPW) and a circular patch configuration, integrated onto a single plane, simplifies the antenna's structure while ensuring consistent impedance, which is vital for broadband applications. The employment of high-quality materials such as FR4 for the substrate and copper for the patch and ground plane has optimized the antenna's performance characteristics, balancing cost-effectiveness with high electrical conductivity, which is essential for minimizing resistive losses. Employing high-conductivity copper for the patch and ground components minimized resistive losses, which is reflected in the exemplary reflection coefficient measurements of -24.7475 dB at 2.4 GHz, -44.8216 dB at 4.9 GHz, and -40.3836 dB at 6.3 GHz. These values indicate a robust impedance matching across the antenna's operational bands, essential for effective signal transmission and reception in 5G networks.

Simulated and experimental results have verified the antenna's capability to maintain excellent reflection coefficients across its operational bandwidth, demonstrating significant gains and effective power transfer. This research contributes significantly to the field of antenna design, particularly for applications requiring wide bandwidth and high gain. The innovative approaches adopted in this study, including the use of a modified ground plane and a CPW feed, set a precedent for future designs in high-frequency wireless communication technologies. The findings not only enhance our understanding of microstrip antenna capabilities but also pave the way for further innovations in 5G antenna technology.

References

[1] Touko Tcheutou Stephane Borel, and Rashmi Priyadarshini, "A Circular Slotted Patch Antenna with Defected Ground Structure for 5G Applications," *International Journal of Engineering Research & Technology*, vol. 11, no. 10, pp. 221-225, 2022. [Google Scholar] [Publisher Link]

[2] Huy Hung Tran, and Tuan Tu Le, "Ultrawideband, High-Gain, High-Efficiency, Circularly Polarized Archimedean Spiral Antenna," *AEU - International Journal of Electronics and Communications*, vol. 109, pp. 1-7, 2019. [CrossRef] [Google Scholar] [Publisher Link]

[3] Raja Meganathan, and Saravanakumar Rengaraj, "Novel Annular Seven Tooth Antenna Compare Its Gain and Return Loss with Circular Patch Antenna for Mobile Navigation," *Bulletin of Electrical Engineering and Informatics*, vol. 12, no. 5, pp. 2887-2894, 2023. [CrossRef] [Google Scholar] [Publisher Link]

[4] G. Shankara Bhaskara Rao et al., "Design and Simulation for 8-Shape 2x4 Slotted Array Antenna Using Ultra Wideband Applications," *International Journal of Computer Engineering in Research Trends*, vol. 10, no. 1, pp. 21-27, 2023. [CrossRef] [Publisher Link]

[5] M. Al-Mihrab et al., "A Compact Size Multiband Printed Monopole Antenna with Triple Sense Circular Polarization for Wireless Applications," *Journal of Optoelectronics and Advanced Materials*, vol. 22, no. 9-10, pp. 483-494, 2020. [Google Scholar] [Publisher Link]

[6] Noor Raheem, and Nidal Qasem, "A Compact Multi-Band Notched Characteristics UWB Microstrip Patch Antenna with a Single Sheet of Graphene," *TELKOMNIKA Indonesian Journal of Electrical Engineering*, vol. 18, no. 4, pp. 1708-1718, 2020. [CrossRef] [Google Scholar] [Publisher Link]

[7] Kin-Fai Tong, and Ting-Pong Wong, "Circularly Polarized U-Slot Antenna," *IEEE Transactions on Antennas and Propagation*, vol. 55, no. 8, pp. 2382-2385, 2007. [CrossRef] [Google Scholar] [Publisher Link]

[8] Nada N. Tawfeeq, "Size Reduction and Gain Enhancement of a Microstrip Antenna Using Partially Defected Ground Structure and Circular/Cross Slots," *International Journal of Electrical and Computer Engineering*, vol. 7, no. 2, pp. 894-898, 2017. [CrossRef] [Google Scholar] [Publisher Link]

[9] R. Kalaiyarasan, G. Nagarajan, and R. Senthil Kumaran, "Design and Implementation of an Efficient Sierpinski Carpet Fractal Antenna for 2.45 GHZ Applications," *SN Computer Science*, vol. 4, 2023. [CrossRef] [Google Scholar] [Publisher Link]

[10] R.V.S. Ram Krishna, Raj Kumar, and Nagendra Kushwaha, "A Circularly Polarized Slot Antenna for High Gain Applications," *AEU - International Journal of Electronics and Communications*, vol. 68, no. 11, pp. 1119-1128, 2014. [CrossRef] [Google Scholar] [Publisher Link]

[11] Shaktijeet Mahapatra, Sarmistha Satrusallya, and Mihir Narayan Mohanty, "A Circular Ultra-Wideband Antenna for Wearable Applications," *Advances in Intelligent Computing and Communication*, pp. 532-536, 2020. [CrossRef] [Google Scholar] [Publisher Link]

[12] Steven Shichang Gao, Qi Luo, and Fuguo Zhu, *Circularly Polarized Antennas*, Wiley-IEEE Press, pp. 1-328, 2014. [Google Scholar] [Publisher Link]

[13] Praveen Kumar Malik, Sanjeevikumar Padmanaban, and Jens Bo Holm-Nielsen, *Microstrip Antenna Design for Wireless Applications*, 1st ed., CRC Press, pp. 1-352, 2021. [CrossRef] [Google Scholar] [Publisher Link]

[14] John D. Kraus, Ronald J. Marhefka, and Ahmad S. Khan, *Antennas and Wave Propagation*, McGraw-Hill Education, 2010. [Google Scholar] [Publisher Link]

[15] Vinod H. Patil et al., "A Testbed Design of Spectrum Management in Cognitive Radio Network Using NI USRP and LabVIEW," *International Journal of Innovative Technology and Exploring Engineering*, vol. 8, no. 9S2, pp. 257-262, 2019. [CrossRef] [Google Scholar] [Publisher Link]

[16] Zhi Ning Chen et al., *Handbook of Antenna Technologies*, 1st ed., Springer Singapore, 2016. [CrossRef] [Google Scholar] [Publisher Link]

[17] Indumathi Ganesan, and Paulkani Iympalam, "Design of Ultra Wideband Circular Slot Antenna for Emergency Communication Applications," *e-Prime - Advances in Electrical Engineering, Electronics and Energy*, vol. 6, pp. 1-9, 2023. [CrossRef] [Google Scholar] [Publisher Link]

[18] Abdullah Baz et al., "Miniaturized and High Gain Circularly Slotted 4×4 MIMO Antenna with Diversity Performance Analysis for 5G/Wi-Fi/WLAN Wireless Communication Applications," *Results in Engineering*, vol. 20, pp. 1-12, 2023. [CrossRef] [Google Scholar] [Publisher Link]

[19] Saad Hassan Kiani et al., "Side-Edge Dual-Band MIMO Antenna System for 5G Cellular Devices," *AEU - International Journal of Electronics and Communications*, vol. 173, pp. 1-10, 2024. [CrossRef] [Google Scholar] [Publisher Link]

[20] Leena Ukkonen et al., "Performance Comparison of Folded Microstrip Patch-Type Tag Antenna in the UHF RFID Bands within 865-928 MHz Using EPC Gen 1 and Gen 2 Standards," *International Journal of Radio Frequency Identification Technology and Applications*, vol. 1, no. 2, pp. 187-202, 2007. [Google Scholar] [Publisher Link]

[21] Rabindranath Bera, Subir Kumar Sarkar, and Swastika Chakraborty, "Advances in Communication, Devices and Networking," *Proceedings of ICCDN*, 2018. [CrossRef] [Google Scholar] [Publisher Link]

[22] Lei Zhang, Qian-Qian Li, and Hai-Feng Zhang, "A Wideband and High-Gain Circularly Polarized Reconfigurable Antenna Array Based on the Solid-State Plasma," *Engineering Science and Technology, an International Journal*, vol. 48, pp. 1-16, 2023. [CrossRef] [Google Scholar] [Publisher Link]

[23] Vinod H. Patil, and Shruti Oza, "Green Communication for Power Distribution Smart Grid," *International Journal of Recent Technology and Engineering*, vol. 8, no. 1, pp. 1035-1039, 2019. [Google Scholar] [Publisher Link]

[24] Mary Swarna Latha Gade et al., "Design of Circular Microstrip Patch Antenna and Its Simulation Results," *Journal of Advanced Research in Dynamical and Control Systems*, vol. 9, no. 4, 230-239, 2017. [Google Scholar]